

CHROMSYMP. 2066

High-performance liquid chromatography of amino acids, peptides and proteins

CIX^a. Investigations on the relation between the ligand density of Cibacron Blue immobilized porous and non-porous sorbents and protein-binding capacities and association constants^b

H. J. WIRTH, K. K. UNGER^c and M. T. W. HEARN*

Department of Biochemistry, Monash University, Clayton, Victoria 3168 (Australia)

ABSTRACT

A porous silica of nominal 5 μm particle diameter and 30 nm pore size (Nucleosil 300-5) and a non-porous silica of nominal 1.5 μm particle diameter were activated with 3-mercaptopropyltriethoxysilane (MPTS), followed by the immobilization of the triazine dye, Cibacron Blue F3GA. Various biomimetic dye sorbents with graduated ligand densities between 1 $\mu\text{mol}/\text{m}^2$ and 0.01 $\mu\text{mol}/\text{m}^2$ were prepared. The capacities and the association constants associated with the binding of lysozyme to these sorbents were determined by frontal analysis experiments [*J. Chromatogr.*, 476 (1989) 205–225].

Due to the ability of the Cibacron Blue F3GA-modified silicas to act as mixed mode coulombic and hydrophobic interaction sorbents and the highly charged nature of the surface structure of lysozyme (pI 11), two mobile phase conditions were examined. In one case a 0.1 M phosphate buffer, pH 7.8, was used as the equilibration and loading buffer, in the second case 1 M sodium chloride –0.1 M phosphate buffer, pH 7.8 was employed as the equilibration and loading buffer to monitor the influence of ionic interactions. The elution was performed in each case with a 2.5 M potassium thiocyanate solution.

With the porous silica dye sorbents and 1 M NaCl present in the loading buffer, the highest capacity was achieved when Cibacron Blue F3GA was immobilised to the level of 0.1 $\mu\text{mol}/\text{m}^2$. In the case of the non-porous silica dye sorbents, the maximum protein capacity was achieved when 0.5 $\mu\text{mol}/\text{m}^2$ dye were immobilised onto the support. Evaluation of the frontal breakthrough curves confirmed that the kinetics of adsorption of lysozyme onto the non-porous sorbent were substantially faster than the adsorption of lysozyme onto the porous sorbent due to the absence of pore diffusion effects in case of the non-porous

^a For Part CVIII, see ref. 20.

^b It is a great pleasure for the authors to dedicate this publication to Lloyd Snyder. As a towering influence over the chromatographic science, Lloyd has provided an incisive and rigorous scientific focus to many areas of research development throughout his distinguished career. His insight has been a catalyst to innumerable conceptual and practical developments some of which the authors have employed in their own studies. The authors warmly acknowledge Lloyd's monumental scientific accomplishments, his stringent advice and generous friendship.

^c On Sabbatical leave from: Institut für Anorganische Chemie und Analytische Chemie, Johannes Gutenberg-Universität, 6500 Mainz, Germany.

support. Furthermore, the adsorption of lysozyme on both sorbents was faster when no salt was added to the loading buffer, indicating that there is either conformational or reorientation effects operating during the specific binding of the protein to the dye ligand, or that the interaction is proceeding through the participation of a second class of binding sites.

The magnitude of the association constants, K_a , for the lysozyme-Cibacron Blue F3GA systems were found to be dependent on the ligand density of the sorbent. With decreasing ligand density, the protein-ligand interaction became stronger, *e.g.* K_a values became larger. These results confirm earlier observations on the effect of ligand steric compression on the affinate-ligand association constant, *e.g.* the protein needs sufficient space to interact with the ligand in an optimum way. This phenomenon was particularly evident in case of the non-porous silica dye sorbents where no pore diffusion effects can occur to obscure or restrict the interaction between the protein and its ligand.

INTRODUCTION

The increasing use of natural and genetically engineered proteins as pharmaceuticals demands the development of high performance separation techniques, which are able to purify the specific protein rapidly and to a very high purity without destroying its biological activity. In order to achieve product efficiencies at process scale, these purification methods must be able to cope with multistage procedures operating under volume and/or concentration overload conditions. At the other end of the separation spectrum, the analytical separation of specific proteins or other bioproducts at trace levels represent the constant challenge for advanced modes of quality control procedures.

Recently, affinity chromatography based on mechanically stable supports has emerged as a powerful tool for the separation of biopolymers under both analytical- as well as preparative-scale conditions. Traditionally, soft polymeric gels such as agarose, cellulose, or polymethacrylate have been used to prepare affinity sorbents. During the last few years however a growing number of investigators [1-8] have turned their attention to the application of microparticulate porous silicas as supports for the development of high-performance affinity sorbents.

The maintenance of the biological activity of a protein during the separation is the essential objective of affinity chromatography as well as all other modes of adsorption chromatography. Preservation of bioactivity can be achieved by ensuring that the contact time between the support material and the protein of interest in the biological sample is minimized. One way this can be achieved is to employ very rapid separation times based on non-porous sorbents. In our previous studies [6,7] the advantages in analytical and semi-preparative biospecific affinity chromatography of monodisperse, non-porous silicas compared with porous silica-based supports or soft gels were documented.

In conventional laboratory scale biomimetic and biospecific affinity chromatography, separation selectivity is traditionally optimised, *i.e.* a ligand of requisite association constant, K_a , is selected, in preference to the optimisation of separation efficiency. In both process applications and ultramicroanalytical applications, the consequences of inappropriate ligand characteristics are very apparent. However, kinetic considerations [9,10] arising from an analysis of mass transport effects associated with the capture rate, the desorption rate, and the zone broadening due to the component diffusion processes, indicate considerable advantages of non-porous sorbents, once a suitable ligand and ligand density has been selected.

In this paper the influence of the ligand density on the kinetics of adsorption, the binding capacities and the association constants of a protein–biomimetic dye sorbent system has consequently been investigated with porous and non-porous silica support particles. In order to evaluate the binding capacity and the association constant of the adsorbate–ligand complex, frontal analysis was used which, as previously documented from this and other laboratories (see, for example, refs. 6, 7, 11–14) represents an accurate method to quantitatively compare different chromatographic adsorption systems. The biomimetic ligand employed was Cibacron Blue F3GA, a triazine dye which has been widely used for the fractionation of NAD-dependent enzymes and many other proteins.

EXPERIMENTAL

Preparation of the sorbents

In the following investigations, a porous silica of nominal 5 μm particle diameter (d_p) and 30 nm pore size (Nucleosil 300-5, Macherey-Nagel, Düren, Germany) and a non-porous silica of nominal $d_p = 1.5 \mu\text{m}$, prepared as described previously [15], were employed.

The modification of the silicas were performed in two steps. In the first step the support was activated [6] with 3-mercaptopropyltriethoxysilane (MPTS), while in the second step the Cibacron Blue F3GA dye molecule was bound to the thiol group of the immobilized silane. The amount of silane needed for the reaction was calculated from the surface area of the support and the concentration of silanol groups on the surface of about 8 $\mu\text{mol}/\text{m}^2$. Since only half of the silanol groups are accessible to the immobilization ligand, this procedure ensured that the silanating reagent was always added in excess. The silanating reaction was carried out in water, adjusted to pH 3.5 with nitric acid. The silica supports were suspended in the solvent, the silane added and the suspension agitated (inversion shaker) at 363 K for 3 h. After the reaction had finished, the silica was washed with water, followed by methanol and dried.

TABLE I

CONDITIONS TO IMMOBILIZE CIBACRON BLUE F3GA ON MERCAPTO-ACTIVATED SILICAS

In case of a ligand density of 1 $\mu\text{mol}/\text{m}^2$ the dye was added to the reaction mixture in 0.5 mole equivalents excess to ensure a maximum ligand density.

Silica	Ligand density ($\mu\text{mol}/\text{m}^2$)	Amount of immobilized dye (mg/g silica)
Nucleosil 300-5	1	160
	0.1	8
	0.01	0.8
Non-porous silica 1.5 μm	1	3.0
	0.5	1.1
	0.2	0.44
	0.1	0.22
	0.01	0.023

The conditions used for the immobilization of Cibacron Blue F3GA are given in Table I. In brief, the MPTS-silicas were suspended in a 0.1 M sodium carbonate buffer, pH 8.2 containing 0.5 M sodium chloride. The dye (1.5 mole equivalents in the case of the maximally covered sorbent and adjusted as appropriate for the sorbents of lower ligand density) was then added and the mixture shaken (inversion shaker) for 24 h at 333 K. Depending on porosity of the support and the final prepared ligand density, the color of the resulting sorbent ranged from deep blue, aquamarine, to a very faint shade of sky blue in colour. Ligand densities were determined as described previously [6,11,12].

The sorbents were packed by the slurry procedure into LiChroCart cartridge columns, which were 19 mm × 4 mm I.D. All frontal analysis experiments were performed at 282 K with an eluent flow-rate of 0.5 ml/min. Protein frontal breakthrough was monitored spectrophotometrically at a detector wavelength of 276 nm.

Equipment and instrumental procedures

The equipment used for the frontal analysis experiments (Fig. 1) consisted of two HPLC pumps (Waters Model 6008; Millipore, Bedford, MA, USA). The first HPLC pump (1) delivered the protein solution while the second pump (2) delivered the elution and the washing buffer. The column (3), a LiChroCart cartridge column 19 × 4 mm, supplied by Merck (Darmstadt, Germany) was connected to the pumps by a 6-way valve (6). The column outlet was attached to a variable-wavelength Waters Model 450 detector (4) and to a Shimadzu chart recorder (5). A LKB Multitemp 2209 thermostat was used to keep the column at a defined temperature.

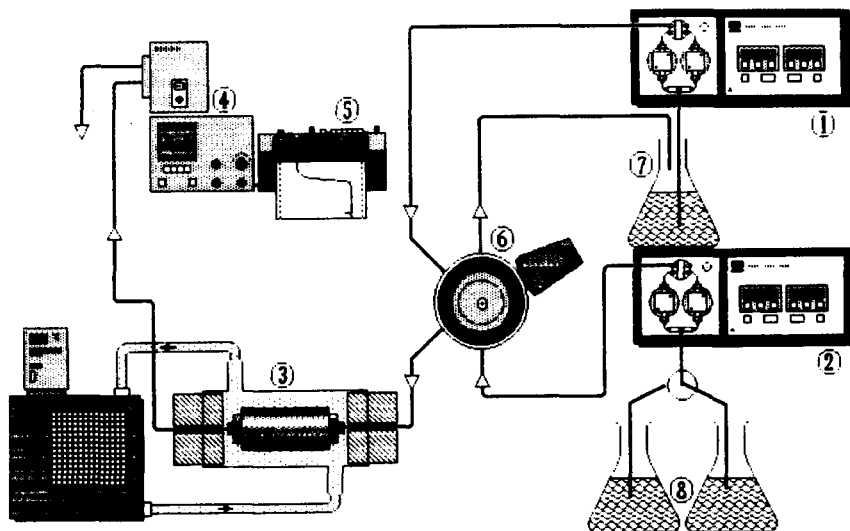


Fig. 1. High-performance liquid chromatography (HPLC) equipment used for frontal analysis experiments. 1 = Pump for the protein solution; 2 = pump for elution and washing buffer; 3 = thermostated column; 4 = UV detector; 5 = chart recorder; 6 = Rheodyne valve; 7 = protein solution; 8 = elution and washing buffer.

Each frontal analysis experiment consisted of three steps. In the first step, the protein solution was pumped through the column until all binding sites were saturated and a constant breakthrough plateau was achieved. In the second step, the protein bound to the column was eluted by adding a competitive ligand or a chaotropic salt to the mobile phase, or by changing the pH value. The elution conditions were designed to be as gentle as possible to retain the biological activity of the protein. In the third step, the column was washed with the reequilibration buffer to remove all components introduced during the elution step. The whole procedure was repeated as multiple replicates ($n > 4$) with the same and different protein concentrations.

Evaluation of the frontal analysis data

Frontal analysis is a method which can evaluate the accessible ligand concentration on the surface of a sorbent as well as the value of the association constant (K_a) between the ligand and the protein. To calculate the breakthrough volume, V_e , the following integral under the breakthrough curve has to be solved.

$$V_e = \frac{1}{M} \int_0^M V dm$$

where

M = initial adsorbate concentration

m = momentary adsorbate concentration at the column outlet

V = volume

The calculation of this integral was done numerically with an "in-house" programme written in Turbo-C for an IBM-compatible personal computer.

The association constant and the accessible ligand concentration were evaluated according to the methods of Nichol *et al.* [16]. The following expression was employed together with appropriate input values derived from the results of the frontal analysis experiments:

$$\frac{1}{V_e - V_0} = \frac{1}{V_0[L]K_a} + \frac{[A]}{V_e[L]}$$

where

V_e = breakthrough volume

V_0 = elution volume of the adsorbate without interaction

K_a = association constant of the adsorbate-ligand complex

$[A]$ = average adsorbate concentration

$[L]$ = accessible ligand concentration

This treatment assumes a first order dependency between the average adsorbate concentration and the reciprocal breakthrough volume. The value for V_0 was determined from the elution volume of non-retarded proteins and was found with the systems used in the present study to be independent of the protein concentration. With the knowledge of V_0 the accessible ligand concentration was then calculated from the slope of the dependency whilst the association constant, K_a , was evaluated from the y-axis intercept.

RESULTS AND DISCUSSION

Studies with the immobilized Cibacron Blue F3GA Nucleosil 300-5 system

Three experimental systems of different ligand density were examined with the surface-modified Nucleosil 300-5 support, namely a dye sorbent with maximal coverage equivalent to $1 \mu\text{mole}/\text{m}^2$, and two dye sorbents with partial coverage of 0.1 and $0.01 \mu\text{mole}/\text{m}^2$, respectively.

In the case where the porous Nucleosil 300-5 silica was modified with the maximum amount of Cibacron Blue F3GA, experimental breakthrough curves were obtained by using a loading buffer with and without $1 M$ NaCl added in order to examine the difference in protein–ligand interactions due to non-specific ionic effects and the effects due to specific biomimetic affinity interactions. The isotherms, corresponding to these experiments, are shown in Fig. 2. In case of the dye sorbents with ligand densities corresponding to 10% and 1% coverage only the loading buffer condition with $1 M$ NaCl added was used to accumulate data on the specific interactions. The adsorption isotherms for these experiments are shown in Figs. 3 and 4.

The values for the accessible ligand concentrations and the association constants for the lysozyme–Cibacron Blue F3GA interactions for these four different experimental conditions were calculated by methods adapted from Nichol *et al.* [16], and are listed in Table II. When $1 M$ sodium chloride was added to the loading buffer in case of the Nucleosil 300-5 dye sorbent with maximum ligand density, the accessible ligand concentration, *i.e.* the amount of immobilised dye ligands which are accessible to lysozyme and which determine the effective binding capacity, q_m , for this adsorbate–ligand system, was decreased by about 48% compared to the salt-free loading buffer condition. For the Nucleosil 300-5 dye sorbent with a ligand density of $0.1 \mu\text{mole}/\text{m}^2$, it is noteworthy that the accessible ligand concentration increased by about 50% compared to the sorbent with $1 \mu\text{mole}/\text{m}^2$ coverage although $1 M$ salt was again added to depress ionic interactions. With further decrease in ligand density to $0.01 \mu\text{mole}/\text{m}^2$,

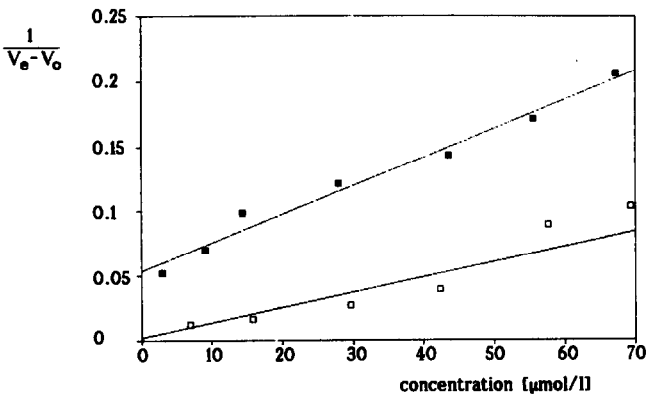


Fig. 2. Adsorption isotherm of lysozyme on Cibacron Blue F3GA-modified Nucleosil 300-5 with maximum ligand density. Mobile phases: □ = $0.1 M$ phosphate buffer pH = 7.9; ■ = $0.1 M$ phosphate buffer with $1 M$ NaCl.

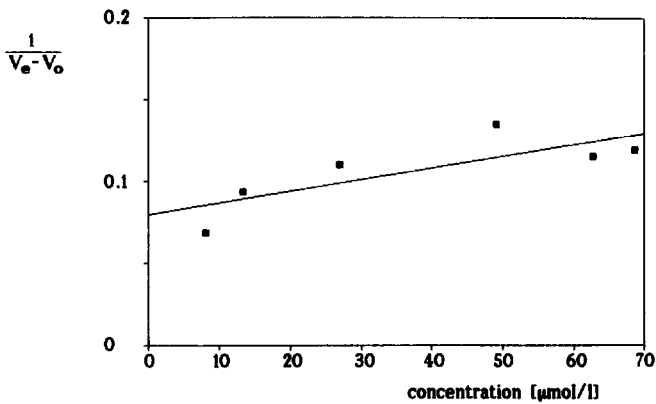


Fig. 3. Adsorption isotherm of lysozyme on Cibacron Blue F3GA-modified Nucleosil 300-5 with $0.1 \mu\text{mol}/\text{m}^2$ ligand density. Mobile phase: $0.1 M$ phosphate buffer with $1 M$ NaCl.

the accessible ligand concentration and thus the capacity decreased as expected to *ca.* 12% of these initial values.

Studies with Cibacron Blue F3GA-immobilized 1.5 μm non-porous silica-lysozyme system

As in the preceding experiments with the porous Nucleosil 300-5 support, the frontal analysis experiments were performed with the non-porous sorbents with and without $1 M$ sodium chloride added to the loading buffer and sorbents of varying ligand coverage ranging from maximum ligand density, equivalent to 1, 0.5, 0.2, 0.1 and $0.01 \mu\text{mole}/\text{m}^2$. The adsorption isotherm of lysozyme on the support with $1 \mu\text{mole}/\text{m}^2$ and a loading buffer without salt added is shown in Fig. 5. When $1 M$ salt was added to the loading buffer, no specific binding could be observed. By decreasing the ligand density to $0.5 \mu\text{mol}/\text{m}^2$, the isotherms shown in Fig. 6 were obtained. Here

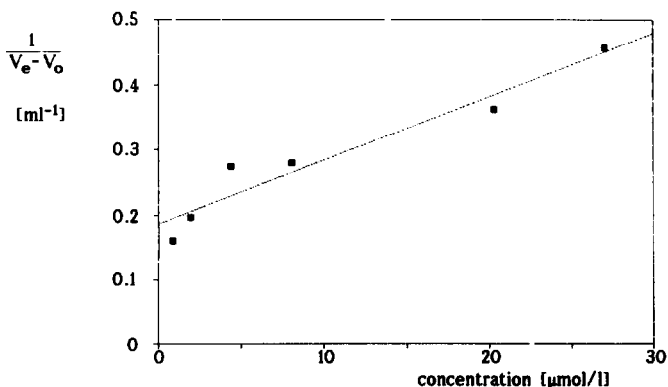


Fig. 4. Adsorption isotherm of lysozyme on Cibacron Blue F3GA-modified Nucleosil 300-5 with $0.01 \mu\text{mol}/\text{m}^2$ ligand density. Mobile phase: $0.1 M$ phosphate buffer with $1 M$ NaCl.

TABLE II

ACCESSIBLE LIGAND CONCENTRATION AND ASSOCIATION CONSTANT OF CIBACRON BLUE-MODIFIED NUCLEOSIL 300-5 AND LYSOZYME AS SUBSTRATE

Ligand concentration ^a ($\mu\text{mol}/\text{m}^2$)	Accessible ligand concentration (μmol)	Association constant ($\cdot 10^7 \text{ mol}^{-1}$)
1	1.77 ± 0.41	36.3 ± 8.4
1	0.91 ± 0.11	4.2 ± 0.5
0.1	1.71 ± 0.41	1.5 ± 0.3
0.01	0.21 ± 0.04	5.2 ± 1.1

^a Mobile phase: 0.1 M phosphate buffer pH 7.8 + 1 M sodium chloride.

the accessible ligand density was in the same range for both specific and non-specific interactions. In Fig. 7 the adsorption isotherms of lysozyme on Cibacron Blue F3GA-modified non-porous silica with a $0.2 \mu\text{mol}/\text{m}^2$ ligand density is plotted. The upper curve corresponding to the frontal analysis experiments with 1 M NaCl added to the mobile phase, shows a non-ideal behaviour of adsorption.

In the frontal analysis experiments with the non-porous dye sorbent with a $0.1 \mu\text{mole}/\text{m}^2$ ligand density only the loading buffer condition of 1 M NaCl was used. The adsorption isotherm for these experiments is shown in Fig. 8. The dye sorbent with $0.01 \mu\text{mole}/\text{m}^2$ of Cibacron Blue F3GA bound to the silica surface showed a very low capacity. Because of the extremely small differences in the values between V_0 and V_e over the corresponding range of protein concentrations, not surprisingly, calculation of the association constant and the accessible ligand concentrations showed significant systematic experimental errors. Nevertheless, the trend of these data showed that the capacity decreased at these very low densities of dye ligands immobilised at the surface of the support, indicating that non-specific interactions with unreached thiol groups were not occurring.

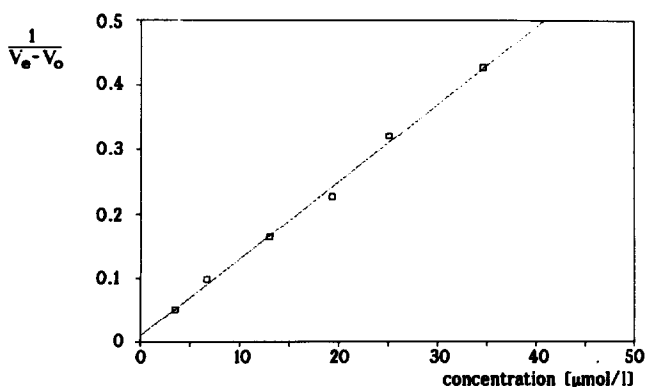


Fig. 5. Adsorption isotherm of lysozyme on Cibacron Blue F3GA-modified non-porous silica with maximum ligand density. Mobile phase: 0.1 M phosphate buffer pH 7.9 without salt added.

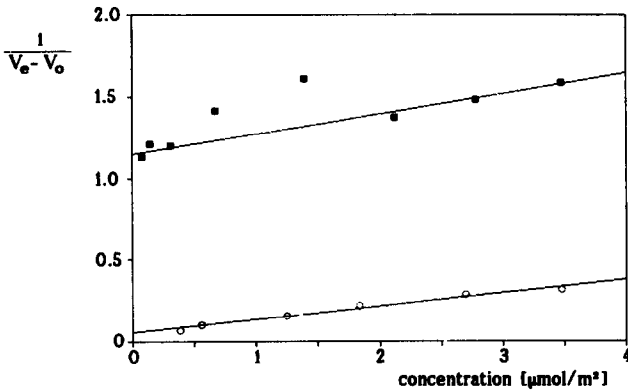


Fig. 6. Adsorption isotherm of lysozyme on $1.5 \mu\text{m}$ non-porous silica with $0.5 \mu\text{mol}/\text{m}^2$ Cibacron Blue F3GA immobilized. Mobile phases: ■ = 0.1 M phosphate buffer pH 7.9; ○ = 0.1 M phosphate buffer pH 7.9 with 1 M NaCl.

Effects of accessible ligand density and ionic strength on association constants and kinetics

In Table III, the accessible ligand concentrations and association constants, calculated from the adsorption isotherms plotted in Figs. 5–8, are tabulated. These data in particular provided comparative information on the effect of high ionic strength conditions on the adsorption process.

The higher capacities, as revealed from the frontal analysis breakthrough curves and isotherm plots for the interaction of lysozyme with the Cibacron Blue F3GA dye sorbents when no salt was added to the loading buffer, reflect the interplay of (at least) three processes occurring during adsorption, namely (i) specific binding involving biomimetic interactions between the dye and unique structural regions of the protein, (ii) non-specific binding involving interaction of the protein to other classes of binding

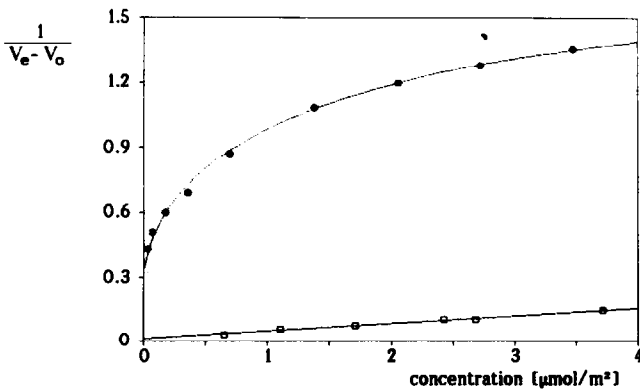


Fig. 7. Adsorption isotherm of lysozyme on $1.5 \mu\text{m}$ non-porous silica with $0.2 \mu\text{mol}/\text{m}^2$ Cibacron Blue F3GA immobilized. Mobile phases: □ = 0.1 M phosphate buffer pH 7.9; ● = 0.1 M phosphate buffer pH 7.9 with 1 M NaCl.

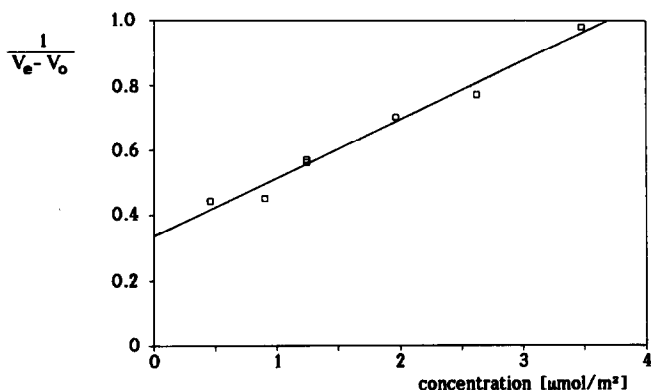


Fig. 8. Adsorption isotherm of lysozyme on $1.5 \mu\text{m}$ non-porous silica with $0.1 \mu\text{mol}/\text{m}^2$ Cibacron Blue F3GA immobilized. Mobile phase: $0.1 M$ phosphate buffer pH 7.9 with $1 M$ NaCl.

sites on the sorbent, and (iii) protein-protein interactions involving conformational or aggregational effects. Protein-protein aggregation is usually interpreted in terms of hydrophobic interactions which increase with increasing ionic strength. Involvement of these hydrophobic effects leads to self-condensation and fractal network formation of proteins in the presence of high salt concentrations. Since a decrease in capacity was observed with increasing salt concentrations, it can be concluded that the origin of these differences in capacity with the low ionic strength loading conditions reside in coulombic, not hydrophobic, effects predominately associated with the silica surface itself. When these non-specific ionic interactions are depressed, the protein prefers to bind via its biomimetic site(s) to the dye ligand. These experimental data further indicate that the kinetics of adsorption become slower under conditions where, in relative terms, fewer of the ligands are utilised, *i.e.* the effective capacity decreases with dye sorbents when the ligand density is high due to steric hindrances.

The decrease in the adsorption kinetics when high salt concentrations are employed in the eluent is particularly evident when the breakthrough curves for the

TABLE III

ACCESSIBLE LIGAND CONCENTRATION AND ASSOCIATION CONSTANT CALCULATED FROM THE ADSORPTION ISOTHERMS USING THE NON-POROUS, $1.5 \mu\text{m}$ d_p SILICA AS SUPPORT

Ligand concentration ($\mu\text{mol}/\text{m}^2$)	Accessible ligand concentration (μmol)	Association constant ($\times 10^6 \text{ mol}^{-1}$)
1^b	0.33 ± 0.02	1.33 ± 0.07
0.5^b	0.043 ± 0.006	45.6 ± 6.8
0.5^a	0.034 ± 0.003	0.10 ± 0.01
0.2^b	0.11 ± 0.01	3.81 ± 0.6
0.2^a	0.015 ± 0.002	0.46 ± 0.07
0.1^a	0.023 ± 0.003	0.53 ± 0.06

^a Mobile phase: $0.1 M$ phosphate buffer pH 7.8 + $1 M$ sodium chloride.

^b Mobile phase: $0.1 M$ phosphate buffer pH 7.8.

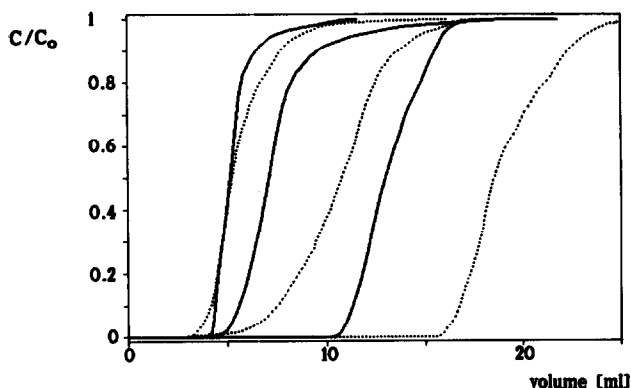


Fig. 9. Comparison of breakthrough curves with specific and non-specific interactions. Breakthrough curves are shown with specific interactions (.....) and ionic interactions (—) for the non-porous dye sorbents of ligand density 1 (right), 0.5 (middle) and 0.2 $\mu\text{mol}/\text{m}^2$ (left). C_0 = Inlet concentration; C = instantaneous concentration.

non-porous silica dye sorbents are compared for specific and non-specific binding. When no salt is added to the mobile phase, the slope of the breakthrough curve becomes substantially steeper (see Fig. 9). A reason for the slower kinetics for the specific binding when salt is present might be the requirement for the protein to undergo a re-orientation or minor conformational change during the binding step. Similar conformational changes have been documented [17,18] for enzyme-substrate binding, antibody-antigen interactions and protein-DNA interactions. This effect is not evident with the porous Nucleosil 300-5 silica sorbents. With these porous sorbents kinetic effects associated with protein transport within the porous structure ("pore" diffusion effects) are superimposed upon the adsorption kinetics. Pore diffusion restrictions represent [19] with these porous sorbents, the rate limiting step for binding with proteins with molecular weights larger than 20 000. The experimental data further confirm the requirement to minimise ligand crowding, *e.g.* surface space is needed for the protein to bind in an optimum way to the immobilised dye. Similar results have been reported [11] for immunoaffinity sorbents. The fact that the value of the association constant increases with decreasing ligand density (see Fig. 10), suggests

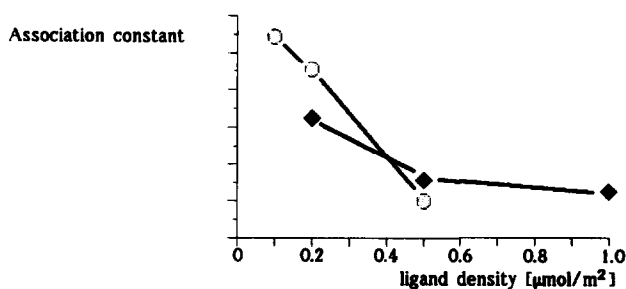


Fig. 10. Relation between the ligand density and the association rate constant with the 1.5- μm non-porous silica modified with Cibacron Blue F3GA. Mobile phase: 0.1 M phosphate buffer with 1 M NaCl added (◆) and without salt added (○).

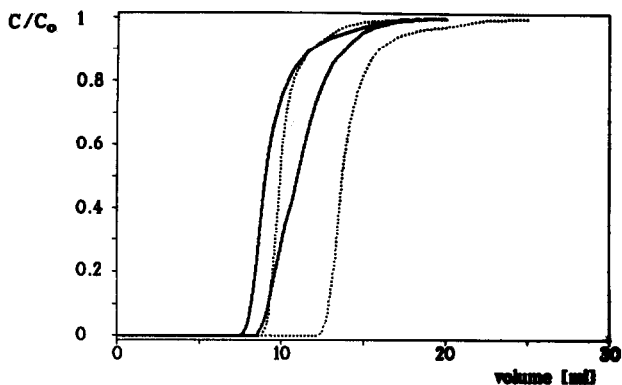


Fig. 11. Comparison of breakthrough curves on porous and non-porous supports. Breakthrough curves are shown for the non-porous (·····) and porous supports (—) eluted with a mobile phase of 0.1 *M* phosphate buffer containing 1 *M* NaCl (right) or without 1 *M* NaCl (left). C_0 = Inlet concentration; C = instantaneous concentration.

that as more space is made available for the protein to bind, in general, the stronger will become the association between the adsorbate and ligand.

Another result evident from these studies is the advantage in using a non-porous compared to a porous silica support for very rapid ultramicroanalytical dye affinity separations. This advantage is easily seen, when the breakthrough curves using the non-porous silica are compared with those using the porous silica (see Fig. 11). When the non-porous silica sorbents were used, the breakthrough curves were much steeper, indicative of faster overall binding kinetics, compared to the corresponding porous silica, whilst all other experimental condition remain unchanged. Although the present study has examined the adsorption behaviour of only a single protein—hen eggwhite lysozyme—similar trends have been observed [10,12] with other proteins and multicomponent protein mixtures in analogous dye affinity systems. These results highlight further the necessity to discriminate the factors which contribute to the adsorption rate. For example, kinetics effects due to additional mass transport mechanisms are operating when a porous support is used, with the kinetic effects due to adsorption often overwhelmed by the mass transfer effects due to pore diffusion. Procedures to discriminate the contributions from film, pore and adsorption transport effects have been reviewed [19] recently. As also noted previously [8–11], and confirmed in this study, examination of the relationship between ligand density and the effective capacity of a sorbent is necessary to optimize an affinity system. This requirement has been found to be especially important when expensive ligands, *e.g.* monoclonal antibodies, are used in biospecific affinity chromatography [11].

ACKNOWLEDGEMENTS

These investigations were supported by Grants from the Australian Research Council and the Monash University Research Excellence Committee.

REFERENCES

- 1 P. O. Larsson, *Methods Enzymol.*, 104 (1984) 212.
- 2 J. Turkova, K. Blaha and K. Adamamova, *J. Chromatogr.*, 236 (1982) 375.
- 3 R. R. Walters, *J. Chromatogr.*, 249 (1982) 19.
- 4 M. T. W. Hearn, *Methods Enzymol.*, 135 (1987) 102.
- 5 K. Nilsson and K. Mosbach, *Methods Enzymol.*, 135 (1987) 65.
- 6 F. B. Anspach, H. J. Wirth, K. K. Unger, P. Stanton, J. R. Davies and M. T. W. Hearn, *Anal. Biochem.*, 179 (1989) 171.
- 7 F. B. Anspach, A. Johnston, H. J. Wirth, K. K. Unger and M. T. W. Hearn, *J. Chromatogr.*, 476 (1989) 205.
- 8 T. Miron and M. Wilchek, *Methods Enzymol.*, 135 (1987) 84.
- 9 A. I. Liapais, B. Anspach, M. E. Findley, J. Davies, K. K. Unger and M. T. W. Hearn, *Biotech. Bioengin.*, 34 (1989) 467.
- 10 M. T. W. Hearn, Q. Mao and A. Johnston, submitted for publication.
- 11 M. T. W. Hearn and J. D. Davies, *J. Chromatogr.*, 512 (1990) 23.
- 12 A. Johnston and M. T. W. Hearn, *J. Chromatogr.*, 512 (1990) 101.
- 13 J. Jacobsen, J. Frenz and Cs. Horváth, *J. Chromatogr.*, 316 (1984) 53.
- 14 K. I. Kasai, Y. Oda, M. Nishikata and S. I. Ishii, *J. Chromatogr.*, 376 (1986) 33.
- 15 G. Jilge, R. Janzen, K. K. Unger, J. N. Kinkel and M. T. W. Hearn, *J. Chromatogr.*, 397 (1987) 71.
- 16 L. W. Nichol, A. G. Ogsten, D. J. Winzor and W. H. Sawyer, *Biochem. J.*, 143 (1974) 435.
- 17 W. F. DeGrado, *Adv. Protein Chem.*, 39 (1988) 51.
- 18 D. M. Brems and H. A. Havel, *Proteins*, 5 (1989) 93.
- 19 A. Johnston, Q. M. Mao and M. T. W. Hearn, *J. Chromatogr.*, 548 (1991) 127.
- 20 R. Janzen, K. K. Unger, W. Muller and M. T. W. Hearn, *J. Chromatogr.*, 520 (1991) 77-93.